MICROSTRUCTURAL CHANGES OCCURRED DURING HOT-DEFORMATION OF SDSS F55 (SUPER-DUPLEX STAINLESS STEEL) ALLOY

Saleh Sabah ALTURAIHI[1], Mohammed Hayder ALLUAIBI[2], Elisabeta Mirela COJOCARU[3], Doina RADUCANU[4]

The paper aims to study the effects induced by thermomechanical processing on the microstructural evolution of the Super Duplex Stainless Steel F55 (SDSS F55). The experimental investigations involved five samples, of identical dimensions, hot deformed at temperatures between (800°C - 1100°C). All samples were deformed by the dead-weight drop method at the same potential energy. The microstructural features of SDSS F55 alloy induced by hot deformation were analyzed using scanning electron microscopy (SEM). The results showed that initial sample presented two stable phases (ferrite (δ) and austenite (γ)), while hot deformation at a temperature between (800°C - 1000°C) induces the appearance of the deleterious sigma (σ) and chi (χ) phases. It was observed that the sigma (σ) and chi (χ) phases are disappearing at hot deformation temperatures above 1000°C.

Keywords: SDSS F55 alloy, stainless steel, microstructure evolution.

1. Introduction

In metallurgy, stainless steel is known as inox steel or inox derived from the French term inoxydable (inoxidizable), it is a steel alloy with a minimum of 10.5% chromium content by mass [1, 2]. Duplex stainless steel (DSS) is the most recent family of stainless steels [3-5]. They are called duplex (or austenitic-ferritic) grades because their metallurgical structure consists of two phases austenite (face-centered cubic lattice) and ferrite (body-centered cubic lattice) in almost equal proportions. They are used due to their good mechanical properties in the as-cast (as-welded condition) and excellent corrosion resistance properties (particularly to stress corrosion cracking) [6, 7]. The duplex microstructure was first described by Bain and Griffiths [8] in 1927, but DSS became commercially

[1] PhD student, Faculty of Material Science and Engineering, University POLITEHNICA of Bucharest, Romania, e-mail: salehsabah2016@gmail.com
[2] PhD student, Faculty of Material Science and Engineering, University POLITEHNICA of Bucharest, Romania, e-mail: mohammed.aluaibi@gmail.com
[3] Eng., Faculty of Material Science and Engineering, University POLITEHNICA of Bucharest, Romania, e-mail: mirela.cojocaru@mdef.pub.ro
[4] Prof., Faculty of Material Science and Engineering, University POLITEHNICA of Bucharest, Romania, e-mail: doina.raducanu@mdef.pub.ro

available in the 1930s. Many advantages are apparent in the DSS in comparison with the austenite steel like higher mechanical strength, superior resistance to corrosion and lower price because of nickel content. Later it was realized that the DSS advantages could be obtained from the use of the DSS in high-stress corrosion cracking environments, while the standard austenitic steels were inappropriate in these environments [9, 10]. Recently was the interest in the DSS alloys as a result of new DSS alloys development have high corrosion resistance induced of the chloride conditions, which is a major problem of concern in many marine and petrochemical applications. On the other hand, the great importance in weldability improving achieved by reducing the carbon content and increasing the nitrogen content.

Thermo-mechanical processing which combines between the deformation and heat treatment, it is very effective for the microstructure control and hence to improve the mechanical properties of metallic materials. For example, in the type of Fe-Cr-Ni DSS alloy, a duplex microstructure consisting of ferrite and austenite in a fine-grained form (1-3 pm) is obtained by the proper thermo-mechanical processing. The duplex microstructure exhibits a superplasticity at elevated temperatures [11-13] and high strength, high fatigue strength and good toughness at room temperature [11, 14, 15]. The changes that emerge in the microstructure which has two phases or duplex microstructure affected by various types of the thermo-mechanical processes. The aim of this paper is to examine the microstructure of Super Duplex Stainless Steel - F55 (SDSS - F55) alloy during thermo-mechanical processing at different temperatures.

2. Materials and Methods

UNS S32760 SDSS - F55 alloy was chosen for the current study having a chemical composition shown in Table 1.

Table 1

The chemical composition of the as-received material

Elem. At.	No.	Line S.	Mass norm. %	Atom abs %	Error % (1 Sigma)	Rel. error % (1 Sigma)
Iron	26	K-Serie	61.25	60.77	1.53	2.56
Cr	24	K-Serie	27.33	29.13	0.72	2.70
Ni	28	K-Serie	6.78	6.40	0.19	2.84
Mo	42	K-Serie	2.71	1.56	0.10	3.63
Tn	74	K-Serie	0.32	0.10	0.03	10.46
Si	14	K-Serie	0.49	0.97	0.05	9.66
Mn	25	K-Serie	0.48	0.48	0.04	7.89
Cu	29	K-Serie	0.50	0.44	0.04	7.53
V	23	K-Serie	0.14	0.15	0.03	21.38
			100.00	100.00		

Five samples were examined in the current study and their dimensions were H/D=1.5 mm (height = 25 mm, diameter = 18 mm); the primary work was to breakdown the material equally in a cylindrical shape using a Lathe machine model (Master 180).

Thermo-mechanical processes

After the samples cutting processes, all samples were subjected to the thermo-mechanical processes. The thermo-mechanical processes consist of a hot deformation process by upsetting (pressing). The first step before the hot deformation process was the furnace operated and temperatures set up between ranges (800ºC - 1100ºC). The furnace should be left for 10 minutes to ensure the creation of a homogeneous environment inside all parts of the furnace. Afterward, each sample has been embedded for 20 minutes within the furnace to distribute the heat uniformly throughout the sample. The final step is to lay the samples that were made at different temperatures individually under the hydraulic press (200 ton). Table 2 shows the dimensions of the samples before and after the deformation process.

The deformation degree of the samples has been estimated from the relation below:

$$\varepsilon = \frac{H-h}{H}\ 100 \tag{1}$$

where:
ε - the deformation degree (%);
H - the initial thickness in (mm);
h - the final thickness in (mm).

Table 2

Dimensions of the samples before and after the deformation

Sample No.	Temperature (°C)	Dimension before upsetting (mm)	Deformation degree (%)	Dimension after upsetting (mm)
1	800	Height = 25 Diameter = 18	46	Height = 13.50 mm D= 27.30 mm Max. D= 20.23 mm Min.
2	900	Height = 25 Diameter = 18	46.4	Height = 13.40 mm D= 27.86 mm Max. D= 19.70 mm Min.
3	1000	Height = 25 Diameter = 18	44.8	Height = 13.80 mm D= 27.90 mm Max. D= 19.13 mm Min.
4	1100	Height = 25 Diameter = 18	46.4	Height = 13.40 mm D= 29.50 mm Max. D= 19.46 mm Min.

Fig. 1 shows the relation between the temperature and the deformation degree which estimated according to Eq. 1.

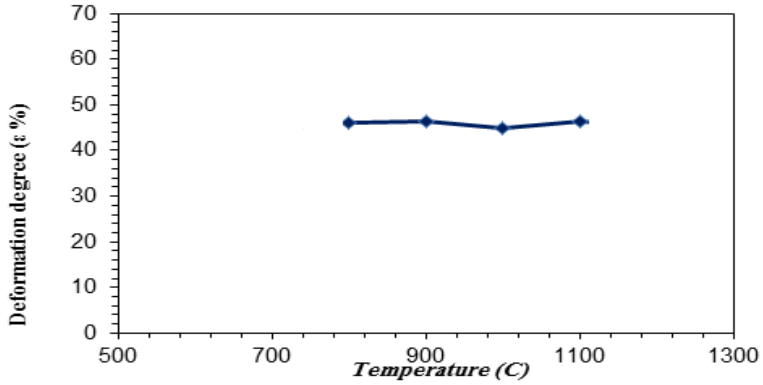

Fig. 1 The relation between the temperature and the deformation degree.

Metallographic Analysis

The five samples were cut for metallographic investigation. The samples were prepared with a very good surface finish using a precision cutter Mekton Micracut 200. Subsequently, all samples were hot mounted using a Buheler SimpliMet mounting press within the cylindrical sampler. Thereafter, all samples were subjected to grinding and polishing using a Mekton DIGIPREP Accura (advanced high-end grinding and polishing system). Eventually, the microstructure was examined using scanning electron microscopy (SEM); model TECSAN VEGA II-XMU.

3. Results and Discussions

Chemical composition (SEM-EDS)

The chemical composition of SDSS - F55 alloy was obtained using SEM. Table 3 shows that SDSS - F55 alloy has two phases are ferrite and austenite (50:50) by weight. Moreover, Fig. 2 shows the areas were chosen for each phase in order to the chemical composition analysis.

Furthermore, Table 4 and Table 5 show the chemical composition of the austenite phase and the ferrite phase respectively. The SEM-EDS spectra were analyzed for both phases and also for SDSS - F55 alloy as shown in Fig. 3.

Table 3

The chemical composition of SDSS - F55 alloy by SEM-EDS

Elem. At.	No.	Line S.	Mass norm. %	Atom abs %	Error % (1 Sigma)	Rel. error % (1 Sigma)

Fe	26	K-Serie	61.25	60.77	1.53	2.56
Cr	24	K-Serie	27.33	29.13	0.72	2.70
Ni	28	K-Serie	6.78	6.40	0.19	2.84
Mo	42	K-Serie	2.71	1.56	0.10	3.63
Tn	74	K-Serie	0.32	0.10	0.03	10.46
Si	14	K-Serie	0.49	0.97	0.05	9.66
Mn	25	K-Serie	0.48	0.48	0.04	7.89
Cu	29	K-Serie	0.50	0.44	0.04	7.53
V	23	K-Serie	0.14	0.15	0.03	21.38
			100.00	100.00		

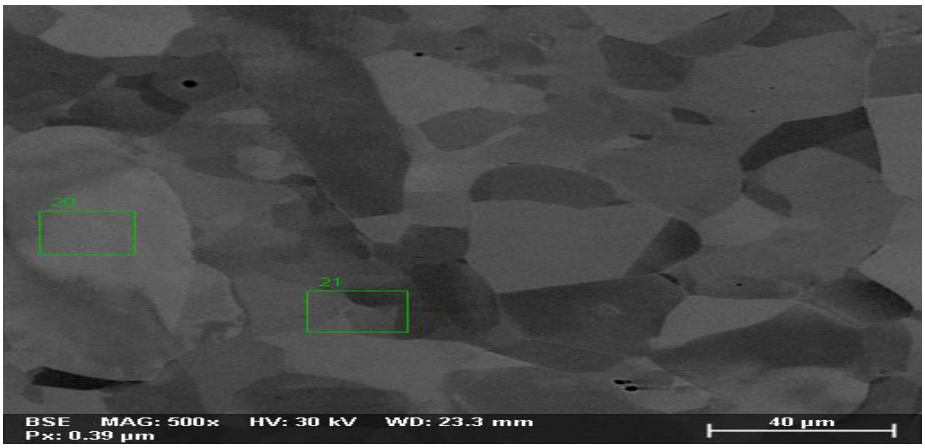

Fig. 2 The selected areas for the chemical analysis of each phase, (20) Austenite, (21) Ferrite.

Table 4

The chemical composition of the austenite phase

Elem. At.	No.	Line S.	Mass norm. %	Atom abs %	Error % (1 Sigma)	Rel. error % (1 Sigma)
Fe	26	K-Serie	62.58	61.85	1.55	2.57
Cr	24	K-Serie	25.72	27.30	0.68	2.72
Ni	28	K-Serie	8.69	8.18	0.24	2.83
Mo	42	K-Serie	1.33	0.76	0.11	8.35
Tn	74	K-Serie	0.03	0.01	0.00	11.83
Si	14	K-Serie	0.34	0.67	0.04	13.23
Mn	25	K-Serie	0.55	0.55	0.04	7.89
Cu	29	K-Serie	0.59	0.51	0.04	7.78
V	23	K-Serie	0.166	0.17	0.03	20.73
			100.00	100.00		

Table 5

The chemical composition of the ferrite phase

Elem. At.	No.	Line S.	Mass norm. %	Atom abs %	Error % (1 Sigma)	Rel. error % (1 Sigma)
Fe	26	K-Serie	60.77	60.41	1.53	2.57

Cr	24	K-Serie	28.50	30.43	0.76	2.71
Ni	28	K-Serie	5.54	5.24	0.16	3.04
Mo	42	K-Serie	3.23	1.87	0.17	5.53
Tn	74	K-Serie	0.43	0.13	0.04	10.08
Si	14	K-Serie	0.45	0.89	0.05	11.06
Mn	25	K-Serie	0.46	0.46	0.04	8.82
Cu	29	K-Serie	0.47	0.41	0.04	9.01
V	23	K-Serie	0.14	0.16	0.03	21.88
			100.00	100.00		

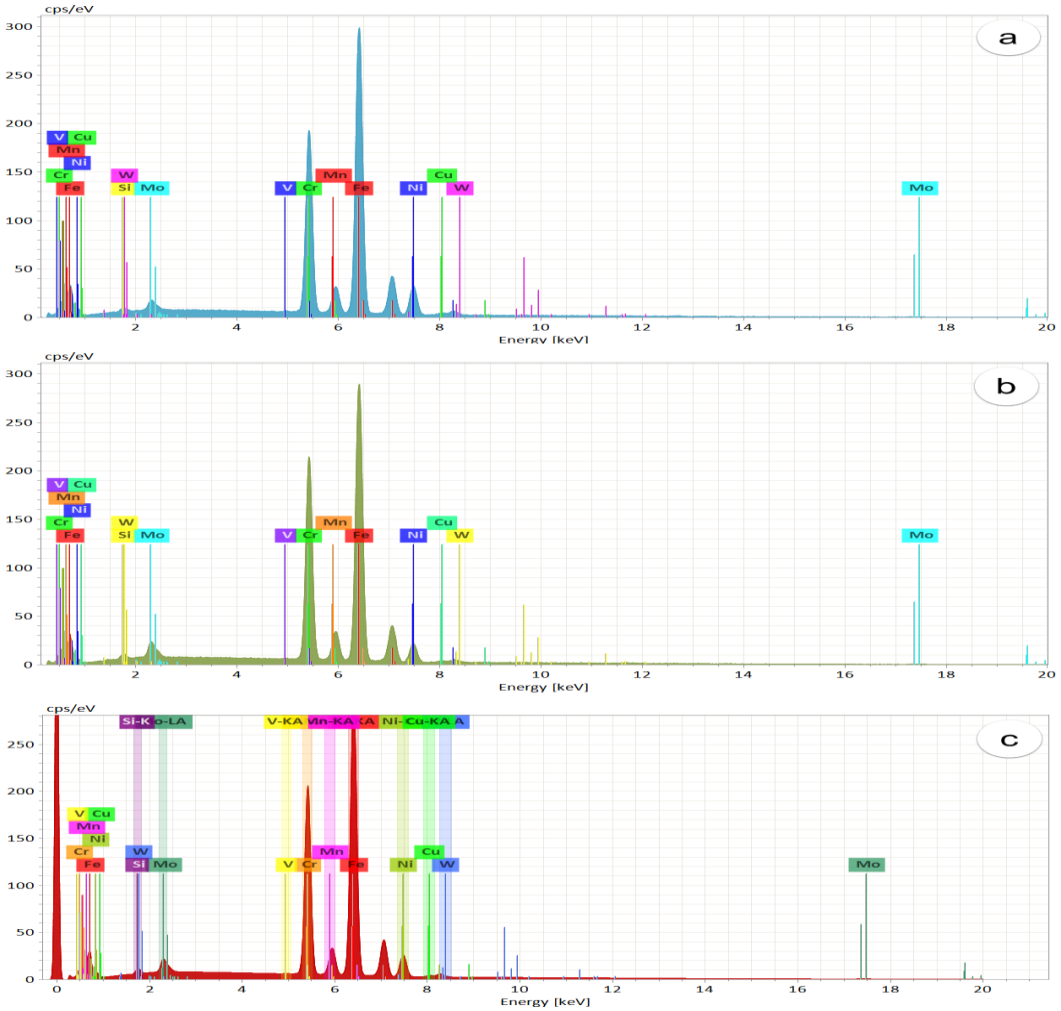

Fig. 3 EDS Spectra; a) Ferrite phase, b) Austenite phase, c) SDSS – F55 alloy.

Microstructures Analyses

The results of the microstructure of sample I (as-received) are shown in Fig. 4. It can be observed is comprised of two phases are austenite 50% and ferrite 50%. The red color refers to the austenite phase and the blue color refers to the ferrite phase as shown in Fig. 4.a while in Figs. 4.b - 4.d show the ferrite grains boundaries and the austenite grains boundaries.

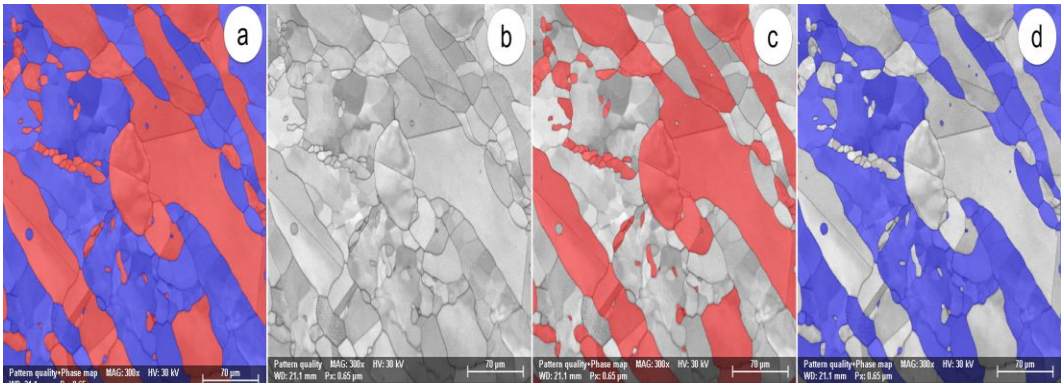

Fig. 4 SEM microstructure analysis of the as-received sample; a) The phases distribution, b) The grains boundaries forms, c) Ferrite deformation, d) Austenite deformation.

The microstructure analysis of sample II which carried out the hot deformation at a temperature of 800°C can be observed in Fig. 5.a; the microstructure contains ferrite phase 54.2% and austenite phase 45.8%. As observed that the austenite phase grains have been elongated. Moreover, in Figs. 5.b - 5.d have also been seen the austenite and ferrite phases have grains more arrangement and distribution as a result of the increase of the temperature.

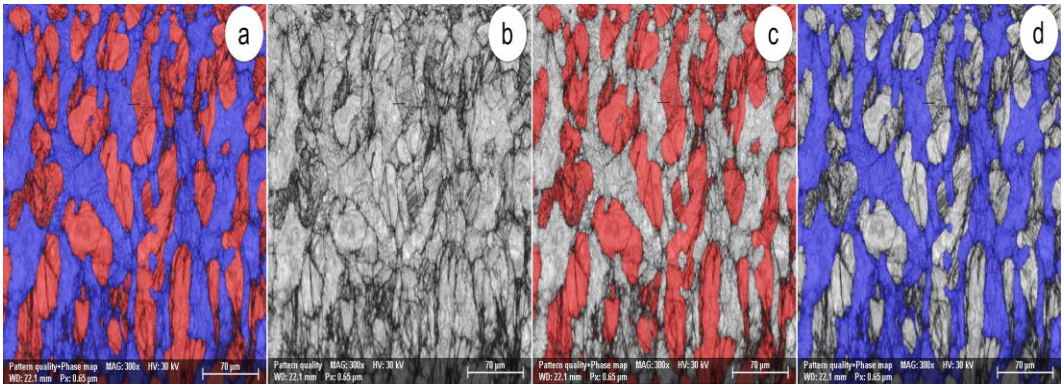

Fig. 5 SEM microstructure analysis of sample II at 800°; a) The phases distribution, b) The grains appearance, c) Ferrite deformation, d) Austenite deformation.

Microstructure analysis of sample III is shown in Fig. 6. It can be observed that an important change in the microstructure which includes a ferrite phase up to 52.3% and austenite phase 40.3%. Furthermore, sigma and chi phases were generated, and their percentages reach 5.19% and 2.25% respectively. As shown in Figs. 6.a - 6.d the thermo-mechanical processing at temperature 900°C makes the mass of the austenite phase less distribution within the ferrite phase matrix. Besides, it was found that in Fig. 6.e was created sigma phase dispersed in the interface between austenite and ferrite phases in addition in Fig. 6.f chi phase only dispersed inside in the ferrite phase. It should be noted that the sigma and chi phases are undesirable because they exhibit brittle behavior.

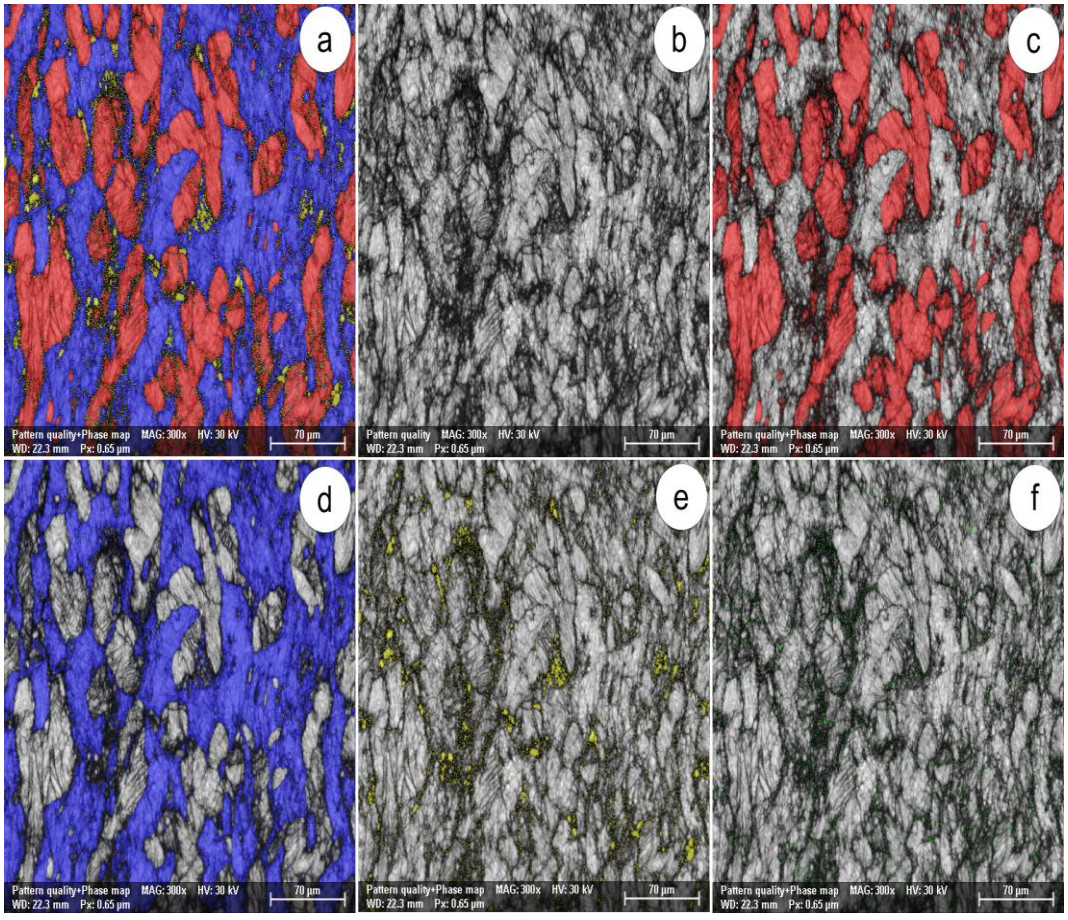

Fig. 6 SEM microstructure analysis of sample III at 900°C; a) The phases distribution, b) The grain boundaries, c) Ferrite Deformation, d) Austenite deformation, e) Sigma phase and his situation in the interface between the ferrite and austenite, f) Chi phase dispersed in the ferrite phase only.

The results of the microstructure analysis for sample IV as shown in Fig. 7. The microstructure presents a significant change in the structure that involves ferrite phase reach to 42.5% and austenite phase 47.1% along with the percentages of sigma and chi phases which appear into the microstructure 2.27% and 8.47% by arrangement. All phases manifesting in Figs. 7.a - 7.f resulting from the thermo-mechanical processing at temperature 1000°C leads to an increase in the content of austenite and chi phases and reduce the concentration of ferrite and sigma phases. It is worth mentioning that the reduced of the ferrite phase content leading to decreased ductility.

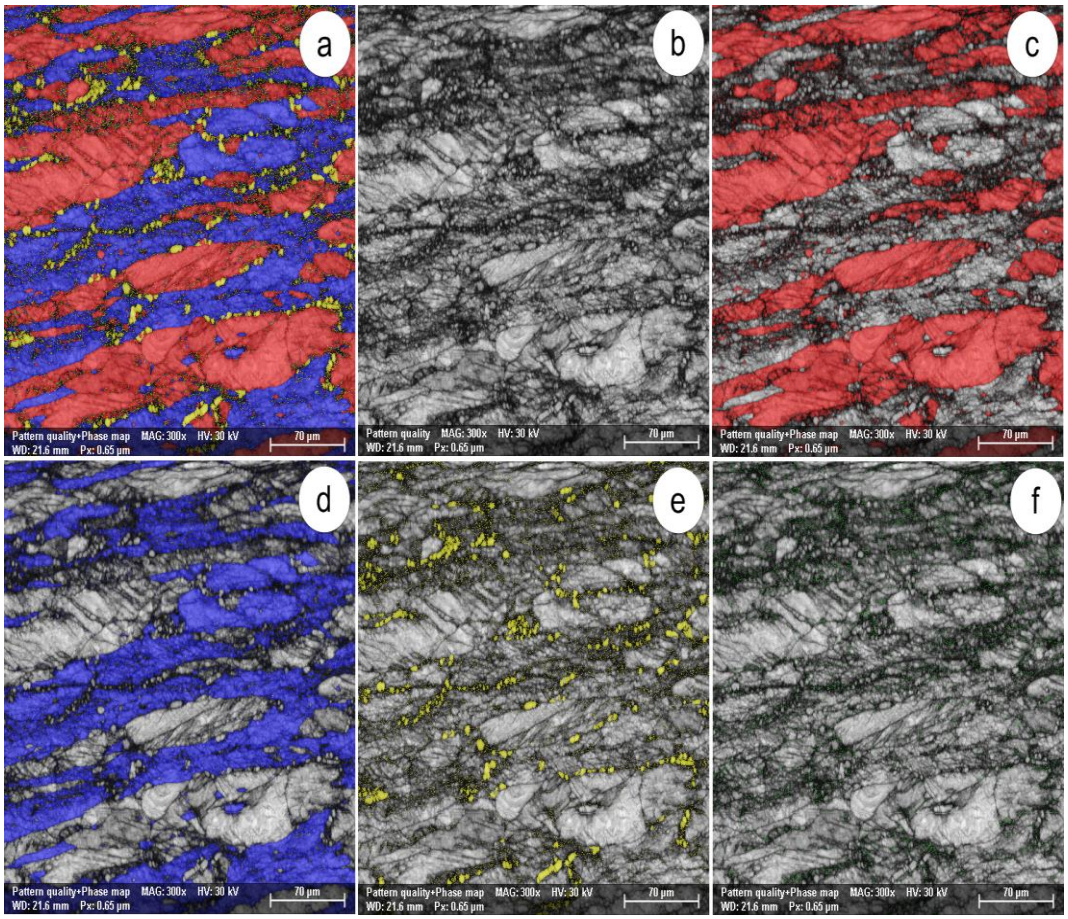

Fig .7 SEM microstructure analysis of sample IV at 1000°C; a) The phases distribution, b) The grain and grain boundaries, c) Ferrite deformation, d) Austenite deformation, e) Sigma phase generated only on the interface between the ferrite and austenite, f) Chi phase dispersed in the ferrite phase only.

Dramatically changes taking place in the microstructure of sample V at high temperature up to 1100°C as shown in Fig. 8. The increase of the temperature resulted in eliminating to unfavorable particles of sigma and chi phases. Fig. 8.a shows the distribution of the ferrite and austenite phases, the contents of the two phases were 58.6% and 41.4% respectively. From Fig. 8.b to Fig. 8.d it can observe the ferrite phase has larger grains more than the austenite phase; in addition, the austenite phase has semi-homogenous distribution into the ferrite matrix.

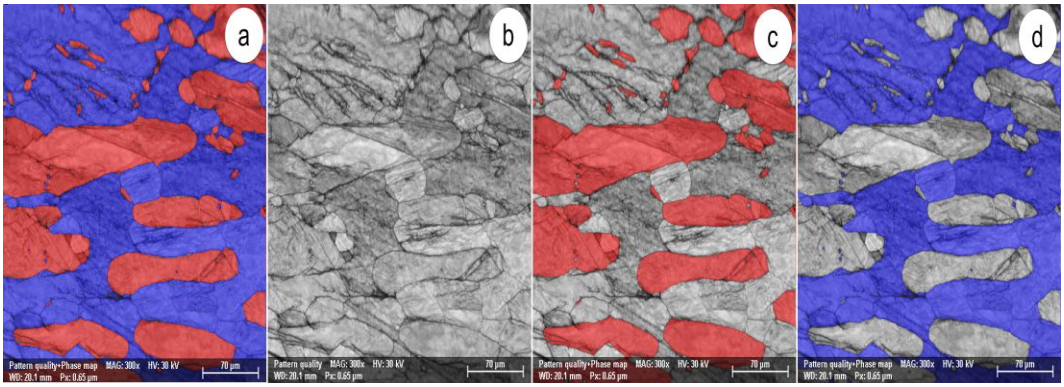

Fig. 8 SEM microstructure analysis of sample V at 1100°C; a) The phases distribution, b) The grain and grain boundaries, c) Ferrite deformation, d) Austenite deformation.

The results of the current paper are meeting dramatically with Cojocaru et al. [16] concerning the chemical composition and the thermo-mechanical processing of SDSS alloy. They have found that the SDSS alloy which subjected to the thermo-mechanical processes between the ranges of temperatures from 800°C to 1000°C resulted to appear the deleterious sigma and chi phases within the microstructure of SDSS alloy. Their results have also shown that the deformation at temperatures above 1000°C eliminate these deleterious phases, and thus improves the microstructure of this alloy.

4. Conclusions

This study comprised different thermo-mechanical processes on Super Duplex Stainless Steel - F55 (SDSS - F55) alloy to explore the effect of these processes on the alloy microstructure under various conditions. It was concluded that the microstructure of SDSS - F55 alloy in the samples which had deformed between the ranges of 800°C - 1000°C showed new phases are sigma (σ) phase and chi (χ) phase, while the sample which had deformed at a temperature 1100°C, can be seen that σ and χ phases disappeared in the microstructure.

Through the metallurgical analysis, the results show that the deformation of the grains of the ferrite (δ) phase is larger and easier than grains of austenite (γ) phase. Alongside, σ phase was generated in the interface between δ phase and γ phase not inside the phases. Moreover, the χ phase was generated only inside the δ phase.

In order to eliminate the deleterious σ and χ phases of SDSS - F55 alloy which it makes to lose the ductility, toughness, stability and corrosion resistance. The thermo-mechanical processes of this alloy must be performed at temperatures more than 1000°C.

R E F E R E N C E S

[1]. *D. Peckner* and *I. M. Bernstein*, Handbook of Stainless Steels, McGraw Hill, New York, 1977, p. 800.

[2]. *P. Lacombe, B. Baroux and G. Beranger*, Les aciers inoxydables, Les Editions de Physique, Les Ulis, France, 1990, p. 1016.

[3]. *J. Chater*, The European market for duplex stainless steels: rapid growth expected, Stainless Steel World, 2010, p. 4.

[4]. *J. Gagnepain*, Duplex stainless steels: success story and growth perspectives, Stainless Steel World, 2008, pp. 31-36.

[5]. *The international molybdenum association (IMOA)*, Practical Guidelines for the fabrication of Duplex Stainless Steels, IMOA, London, UK, 2014, p. 68.

[6]. *S. S. M. Tavares, V. G. Silva, J. M. Pardal and J. S. Corte*, Investigation of stress corrosion cracks in a UNS S32750 superduplex stainless steel, Engineering Failure Analysis, **Vol. 35**, 2013, pp. 88-94.

[7]. *F. Zanotto, V. Grassi, A. Balbo, C. Monticelli and F. Zucchi*, Stress corrosion cracking of LDX 2101 (R) duplex stainless steel in chloride solutions in the presence of thiosulphate, Corrosion Science, **Vol. 80**, 2014, pp. 205-212.

[8]. *E. C. Bain and W. E. Griffiths*, Introduction to the iron-chromium-nickel alloys, Transactions AIME, **Vol. 75**, 1927, pp. 166-213.

[9]. *L. Colombier and J. Hochmann*, Aciers inoxydable aciers réfractaire, Paris, Dunod, **Vol. 1**, 1955, p. 526.

[10]. *C. Edeleanu*, Transgranular stress corrosion in Cr-Ni stainless steels, Journal of the Iron and steel institute, **Vol. 173**, 1953, pp. 140-146.

[11]. *J. O. Nilsson*, Super duplex stainless steels, Journal of Materials Science and Technology, **Vol. 8**, 1992, pp. 685-700.

[12]. *H. W. Hayden, R. C. Gibson, H. F. Merrick and J. H. Brophy*, Superplasticity in the Ni-Fe-Cr System, American Society for Metals (ASM) Transactions Quarterly, **Vol. 60**, No. 1, 1967, pp. 3-13.

[13]. *K. Tsuzaki, H. Matsuyama, M. Nagao and T. Maki*, High-Strain Rate Superplasticity and Role of Dynamic Recrystallization in a Superplastic Duplex Stainless Steel, Materials Transactions, JIM, **Vol. 31**, No. 11, 1990, pp. 983-994.

[14]. *R. C. Gibson, H. W. Hayden and J. H. Brophy*, Properties of stainless steels with microduplex structure, American Society for Metals (ASM) Transactions Quarterly, **Vol. 61**, No. 1, 1968, pp. 85-93.

[15]. *H. W. Hayden and S. Floreen*, The deformation and fracture of stainless steels having microduplex structures, American Society for Metals (ASM) Transactions Quarterly, **Vol. 61**, 1968, pp. 474-488.

[16]. *V. D. Cojocaru, N. Șerban, M. L. Angelescu, M. C. Cotrut, E. M. Cojocaru and A. N. Vintila*, Influence of Solution Treatment Temperature on Microstructural Properties of an Industrially Forged UNS S32750/1.4410/F53 Super Duplex Stainless Steel (SDSS) Alloy, Metals Journal, **Vol. 7**, No. 6, 2017, p. 210.